Research Square

Preprints are preliminary reports that have not undergone peer review.
They should not be considered conclusive, used to inform clinical practice,
or referenced by the media as validated information.

Neuroprotective Effects of Platelet-Rich Plasma in Neonatal Rats with Hypoxic-Ischemic Brain Injury

Tugay Tepe

drtugaytepe@yahoo.com

Cukurova University

Hacer Yapicioglu Yildizdas

Cukurova University

Seyda Erdogan

Cukurova University

Tugba Toyran

Cukurova University

Kübra Akillioglu

Cukurova University

Seda Köse

Cukurova University

Nejat Narli

Cukurova University

Mehmet Satar

Cukurova University

Research Article

Keywords: Platelet-rich plasma, newborn, hypoxic-ischemic brain injury, apoptosis, behavioral tests

Posted Date: November 9th, 2026

DOI: https://doi.org/10.21203/rs.3.rs-11245866/v1

License: This work is licensed under a Creative Commons Attribution 4.0 International License.
Read Full License

Additional Declarations: No competing interests reported.

Neuroprotective Effects of Platelet-Rich Plasma in Neonatal Rats with Hypoxic-Ischemic Brain Injury

*Tugay Tepe[a,b-] 0000-0002-7926-8442- drtugaytepe@yahoo.com.

[a]Department of Pediatrics, Division of Neonatology, Cukurova University Faculty of Medicine, 01330, Adana, Turkey

[b]Department of Physiology, Cukurova University Faculty of Medicine, 01330, Adana, Turkey

Hacer Yapicioglu Yildizdas[a]- 0000-0001-6295-553X- hyapicioglu@cu.edu.tr.

[a]Department of Pediatrics, Division of Neonatology, Cukurova University Faculty of Medicine, 01330, Adana, Turkey

Seyda Erdogan[c]- 0000-0002-4113-2080- seydaer@cu.edu.tr.

[c]Department of Pathology, Cukurova University Faculty of Medicine, 01330, Adana, Turkey

Tugba Toyran[c]- 0000-0001-9135-0265- tugbaolcan@hotmail.com.

[c]Department of Pathology, Cukurova University Faculty of Medicine, 01330, Adana, Turkey

Kübra Akillioglu[b]- 0000-0003-4896-8822- kubraakillioglu@gmail.com.

[b]Department of Physiology, Cukurova University Faculty of Medicine, 01330, Adana, Turkey

Seda Köse[b]- 0000-0001-7386-7578 – ko.seda9613@gmail.com.

[b]Department of Physiology, Cukurova University Faculty of Medicine, 01330, Adana, Turkey

Nejat Narli[a]- 0000-0002-0474-3288- nnarli@cu.edu.tr

[a]Department of Pediatrics, Division of Neonatology, Cukurova University Faculty of Medicine, 01330, Adana, Turkey

Mehmet Satar[a] - 0000-0002-5718-0503- satarm@gmail.com.

[a]Department of Pediatrics, Division of Neonatology, Cukurova University Faculty of Medicine, 01330, Adana, Turkey

Abstract

Hypoxic-ischemic encephalopathy (HIE) remains a leading cause of neonatal morbidity and mortality, and there remains an urgent need for effective therapeutic strategies. This study investigated the neuroprotective effectiveness and long-term benefits of platelet-rich plasma (PRP) therapy in hypoxic-ischemic encephalopathy. Ten-day-old Wistar albino rats were randomized into three groups: PRP (n = 12), HIE (n = 12), and sham (n = 12). With the exception of the Sham group, all animals were subjected to the HIE model. In the PRP group, 5 microliters of PRP per animal was administered as a single intraventricular dose after HI injury, whereas the HIE and sham groups received physiological saline. Five pups from each group were euthanized 72 hours after induction of the model for early-period assessment; the remaining seven pups underwent cognitive-behavioral testing and late-period histological evaluation at 6 weeks of age. Histological evaluations included TTC, TUNEL and IL-1β staining. PRP therapy reduced the infarct size and the number of TUNEL-positive cells, particularly during the late period ($p = 0.01$). Furthermore, PRP treatment attenuated neuroinflammation during both the early and late periods, as evidenced by reduced IL-1β staining ($p=0.01$). Behavioral tests demonstrated that PRP therapy reduced elevated anxiety-like behaviors in HIE. This study demonstrates, for the first time, that PRP therapy may be a promising therapeutic option for HIE in newborns.

Keywords: Platelet-rich plasma, newborn, hypoxic-ischemic brain injury, apoptosis, behavioral tests

Corresponding author: Tugay Tepe, M.D.

Mailing address: Seyhan State Hospital, Erdal Acet Street, 01130, Seyhan, Adana, Turkey

Phone: +90 505 8030859 (Mobile), +90 322 4316001 (Office)

Fax: +90 322 2259329

Email: drtugaytepe@yahoo.com-ttepe@cu.edu.tr

Introduction

Hypoxic-ischemic encephalopathy (HIE) in the newborn period is a condition characterized primarily by neurological impairment resulting from reduced cerebral blood flow and oxygen deprivation. Infants are classified as having mild, moderate, or severe encephalopathy based on the Sarnat Scoring System (Sarnat & Sarnat, 1976). These findings, supported by cranial imaging and amplitude electroencephalography, provide information about the degree of brain damage and the likelihood of neurological sequelae. The incidence of HIE is approximately 2 per 1,000 live births in high-income countries, but it can reach up to 26 per 1,000 live births in developed countries (Douglas-Escobar & Weiss, 2015; Victor et al., 2022). Globally, around one million infants develop moderate to severe HIE annually, resulting in approximately 400,000 babies having a neurodevelopmental impairment (Victor et al., 2022). The pathophysiology of hypoxic-ischemic brain injury (HIBI) is complex, with the primary mechanisms including excitotoxicity, oxidative stress, and inflammation. Ultimately, it leads to neuronal cell death through apoptosis or necrosis. Following HIBI, an initial energy-deficit phase characterized by ATP insufficiency is followed by a latent period during which reperfusion is partially restored. If homeostasis is not adequately restored, a secondary phase of energy deficit develops within 12-72 hours, followed by a third phase of neuronal cell death that continues for days or months (Pedroza-García et al., 2022).

Therapeutic hypothermia (TH) is currently the standard treatment for late preterm and term neonates with moderate to severe types of HIE, initially starting within the first 6 hours of HIBI (Perlman et al., 2010). Although TH is considered the gold standard treatment, approximately half of neonates with moderate or severe HIE treated with TH die or suffer neurological complications (Jacobs et al., 2013). Furthermore, considering constraining factors such as device cost and the limited indications for TH treatment, research on treatments that can be used in conjunction with hypothermia is still ongoing, and an effective approach has not yet been proven (Jerez-Calero et al., 2020; Rüegger et al., 2018; Tsuji et al., 2020; Wu et al., 2022). Consequently, there is a critical need to develop drugs that offer neuroprotection and long-term clinical benefits for infants with HIE. Such therapeutics are essential to serve as either standalone alternatives or adjunctive enhancements to current TH.

Platelet-rich plasma (PRP) is a preparation derived from the centrifugation of donor blood that contains a high concentration of platelets. It encompasses numerous growth factors and cytokines. PRP is regarded as particularly beneficial in angiogenesis, neuroprotection, neurogenesis, and neuroinflammation due to the presence of growth factors, such as platelet-derived growth factor (PDGF), insulin-like growth factor (IGF), vascular endothelial growth factor (VEGF), fibroblast growth factor (FGF), and transforming growth factor-β (TGF-β) (Anitua et al., 2014; Zhang et al., 2015). Experimental evidence demonstrates its efficacy in alleviating the inflammatory response and providing neuroprotection for various neuroinflammatory disorders of the central nervous system (Anitua et al., 2014; Bayat et al., 2020; Borhani-Haghighi & Mohamadi, 2019). Its anti-inflammatory process is mediated by numerous molecules, including IGF-1 and other growth factors, which diminish NF-kB activation in the brain and reduce the expression of nitric oxide, cyclooxygenase, and tumor necrosis factor (Anitua et al., 2015). Other growth factors such as brain-derived neurotrophic factor (BDNF), PDGF, VEGF, IGF-1, and TGF-β have been shown to have antiapoptotic and neuroprotective effects on

mesenchymal stem cells, neurons, and human neural stem cells, either alone or in combination (Emel et al., 2011; Lee et al., 2003; Luo et al., 2012; Rao & Pearse, 2016; Sondell et al., 1999).

This study investigates whether PRP offers neuroprotection in newborn rats with HIBI, specifically focusing on its therapeutic role in hypoxic-ischemic encephalopathy.

Experimental Procedures

Animals

Thirty-six rat pups were provided by University's Experimental Application and Research Center of Health Sciences. Male rat pups, maintained with their mothers and fed with breast milk since birth. Animals were enrolled in the study on postnatal day 10 (PND 10), an age developmentally equivalent to term human infants (Semple et al., 2013). All animals were housed under a 12-hour light/12-hour dark cycle, with room temperature maintained at 21-23°C and humidity maintained at 40-60%. The study only included male rat pups, as female rat pups may interfere with the behavioral assessments during the transition to adulthood (D'Hooge & De Deyn, 2001). The "resource equalization" method was used to determine the number of rats designated for each group (Festing, 2006). Twelve rat pups were assigned to each group using computer-assisted randomization. The groups were as follows: the Sham group (n = 12): a single intraventricular dosage of 5 microliters (5 μL) of physiological saline was given, and then only a skin incision was performed without being subjected to hypoxia or ischemia procedures, Hypoxia-ischemia (HIE) group (n=12): group was subjected to hypoxia-ischemia and administered 5 μL of physiological saline intraventricularly, PRP group (n=12): The group that received 5 μL of PRP intraventricularly. Intraventricular injection was administered over 1 minute using a 25-μL Hamilton syringe (Bonaduz, Switzerland). The dosage was determined based on previous studies in the literature (Miura et al., 2006). PRP Donor Group (n=6): adult males were enrolled and used for homologous PRP preparation. Five pups from each group were euthanized 72 hours after induction of the HIE model, and their brain tissues were collected for early-period analysis. The remaining seven pups underwent cognitive-behavioral tests at 6 weeks of age (adulthood). Body weights were measured daily using a digital scale accurate to 0.1 grams. Humane euthanasia was considered appropriate in cases of significant weight loss, inability to obtain the dam's dairy products, food, or water, or signs of extreme stress during the follow-up period. One rat pup in the PRP group died following the intraventricular injection and was excluded from subsequent analyses.

Animal model of HIE

Unilateral (left) carotid artery ligation was performed following inhalation of isoflurane (POLIFARMA, Tekirdag, Türkiye) (beginning at 4% and then maintained at 1.5%) to induce the HIE model. Subsequently, the animals were exposed to a gas mixture of 8% oxygen and 92% nitrogen for 90 minutes inside a temperature-controlled hypoxic chamber at 34-36 °C aiming to implement Rice-Vanucci's hypoxia-ischemia model (Rice et al., 1981). The rat tails were dyed intradermally using a microneedle (Dr.Pen A6, EKAI tech, Guangzhou, China). Rat pups were returned to their mothers for 30 minutes after the procedure. Subsequently, the prepared PRP treatment was administered intraventricularly over 1 minute via a stereotaxic device (Stoelting, USA) using a Hamilton syringe equipped with a micro-syringe pump. Coordinates targeting the left lateral ventricle (1.0 mm posterior to bregma, 1.5 mm lateral to the sagittal suture, and 3.0 mm ventral to the skull surface) were determined using a rat brain atlas. Injection accuracy was initially confirmed via Evans blue dye administration

in an additional pilot pup not included in the study cohort. The sham group and the HIE group received a single intraventricular dose of 5 µL/animal of physiological saline. At 72 hours after induction of the HIE model, five pups from each experimental group were euthanized under isoflurane anesthesia, and their brain tissues were collected for early-period histological assessment. The remaining seven pups in each group were maintained until 6 weeks of age. Following cognitive and behavioral testing, animals were euthanized for histological evaluation. Researchers who were blind to group allocation performed the surgical procedures, treatment administration, and animal assignment to experimental groups. The intraventricular injections (PRP or saline) were given by one researcher, the procedures were carried out by another, and the data analysis was done by a third researcher. Researchers that were blind to the experimental conditions performed statistical analysis, behavioral testing, pathological evaluation, and image quantification. All protocols in this study were approved by the Ethics Committee of the Medical and Experimental Research Center at University's Faculty of Medicine (approval number 2021-05).

PRP preparation

Six adult male Wistar Albino rats were randomly selected for PRP preparation. Approximately 8 ml of blood was obtained from the right ventricle of each rat's heart while under isoflurane anesthesia. Blood samples were collected into PRP tubes containing 3.20% sodium citrate (VACURESA PRP Kit, Diasera, Izmir, Türkiye). The sample in the tube was then centrifuged at 2500 g for 10 minutes (Thermo Scientific Heraeus Multifuge 3SR, U.S.A.) according to the manufacturer's instruction. Two milliliters of PRP were carefully collected from the plasma layer above the erythrocyte pellet at the bottom of the tube, carefully avoiding the leukocyte-rich buffy coat. Platelet counts in PRP and the initial blood sample were measured and recorded using an automatic counter (The Exigo hematology analyzer, Sweden). The platelet concentration in PRP should be at least three-fold higher than that in whole blood. In our measurements, the baseline whole blood platelet count was 179 x 10^3 /µL, whereas the final PRP preparation yielded a platelet count of 675 x 10^3 /µL, achieving a 3.77-fold concentration. Consequently, the 5 µL intraventricular dose administered to the PRP group contained approximately 3.37 x 10^6 viable platelets.

Histopathological study

Pathological analysis was performed in the Department of Pathology, University Faculty of Medicine. All subsequent procedures including behavioral testing, image quantification, and statistical analysis were also performed by investigators blinded to the treatment groups.

Triphenyl tetrazolium chloride (TTC) and hematoxylin-eosin staining

The collected brain tissues were washed in normal saline at room temperature and then cut into 2-mm sections from the olfactory compartment to the cerebellum. The sections were placed in a saline solution containing 2% TTC (Merck, Darmstadt, Germany) and incubated for 15 minutes at 37 °C. The tissues were then rinsed with phosphate-buffered saline to remove the TTC solution. The sections were fixed in a 4% formaldehyde solution at 4°C for 24 h. Macroscopically, infarcted regions were pale-white, while normal regions exhibited a pink-red color. Infarct areas were quantified using image analysis software (Image-Pro Plus 5.1), and edema-adjusted absolute infarct areas were calculated using the following formula: edema-adjusted infarct area (IEA) = absolute unadjusted infarct area (I) x (contralateral hemisphere area/ ipsilateral hemisphere area). The final volume of the

infarct was obtained by multiplying the thickness of the slice and summing across all slices using the Reglodi method (Nouraee et al., 2019; Reglodi et al., 2002).

IL-1 β staining

For immunohistochemical assessment, paraffin-embedded coronal brain sections were cut at a thickness of 5 μm and rehydrated through an alcohol series of 90%, 75%, and 50%. Sections were stained with IL-1β antibody (rabbit polyclonal antibody, PO1584, 1:400 dilution; Bioss, Boston, USA) using a Ventana BenchMark XT automated immunohistochemistry instrument. Hematoxylin was used as the counterstain, and lymph node tissue was used as a positive control. IL-1β immunostaining was evaluated in the ipsilateral hemisphere, focusing on the peri-infarct cortical and subcortical regions identified with reference to TTC-stained parallel sections. Sections obtained at corresponding coronal levels were evaluated across all animals to ensure anatomical comparability. The prepared sections were examined using an Olympus microscope at ×400 magnification. Within each section, the region showing the highest IL-1β staining was selected, and the percentage of positively stained area within this region was quantified using Image-Pro Plus 5.1 image analysis software. Data were expressed as the percentage (%) of IL-1β-positive stained area.

TUNEL (Terminal deoxynucleotidyl transferase dUTP nick end labeling) staining

In accordance with the manufacturer's instructions, TUNEL staining was performed to detect DNA strand breaks associated with cell death (TUNEL Assay Kit-HRP-DAB, ab206386, Merck, USA). After a one-hour incubation at 60°C and subsequent deparaffinization with xylene for 15 minutes, coronal brain sections (5 μm thick) were incubated with proteinase K for 30 minutes at room temperature. Sections were washed in phosphate-buffered solution and exposed to the terminal deoxynucleotidyl transferase reaction mixture for one hour at 37°C. 3,3-Diaminobenzidine tetrahydrochloride and methyl green were used as the chromogen and counterstain, respectively. Tonsil sections were used as a positive control. TUNEL-positive neurons were counted separately in each hemisphere. Quantification was performed by averaging the number of TUNEL-positive cells across five ischemic regions spanning the parietal cortex, hippocampus, and prefrontal cortex. The same staining protocol and quantification approach were applied at both the early and late timepoints. Data were expressed as the number of TUNEL-positive neurons.

Behavioral tests

The open field (OF) test was used to assess their locomotor ability at six weeks of age, while the Morris water maze (MWM) test was used to assess learning and memory of the seven remaining rats in each group.

Open field test

The open-field structure is constructed of black plexiglass, measures 70 × 70 × 30 cm, and has 1-cm-thick walls and an open top. The rats were placed in a corner of the apparatus, and their behavior was recorded for 5 minutes with a video camera positioned 2.5 m above the center of the field. The light intensity and room temperature were set to 100 lumens and 22 ± 1°C, respectively. Following this, the distance traveled by the rats in the open area, the time spent in the center of the apparatus, and the latency to first enter the center were scored using the ETHOVISION XT computer program, while the frequencies of rearing and defecation were scored manually. In the OF test, rats' anxiety, stress levels, and locomotor activity were evaluated.

Morris water maze test

The Morris water tank is cylindrical, with a diameter of 140 cm and a depth of 45 cm. Although 140 cm is smaller than standard adult tanks, it is appropriate for the body size and swimming capacity of 6-week-old rats. It consists of galvanized sheet metal and has a black interior. There is a mobile escape platform inside the pool that measures 27 cm in height and 10 cm in diameter during experiments. During the experiments, the pool was filled with opaque tap water until the water level reached 1 cm above the platform. The water temperature was set to 21 ± 1 °C. To provide spatial cues to the rats swimming in the pool, black geometric shapes, contrasting with the light-colored walls, were placed on the laboratory walls within the rats' field of vision. The light in the pool has been set to 150 lx. The MWM training trials and final-day tests were used to assess rats' spatial learning and memory. Rats in MWM underwent training trials four times daily for five consecutive days. In each trial, rats were released into the pool from any of the four hypothetical quadrants, and were allowed to swim for 90 seconds to find the escape platform. When the rats reached the platform, they were kept there for 15 seconds before being removed from the pool. During training trials, if rats failed to locate the platform within 90 seconds, they were manually guided to the platform to learn its spatial location and were then kept on it for 15 seconds before being removed from the pool. The platform's position was kept fixed in the same quadrant throughout all trials. Between training trials, rats were kept in their cages for 30 seconds at an appropriate room temperature. On the final day of testing, the platform was removed from the pool, and the rats were released from the quadrant opposite that in which the platform had been located before its removal. During the test, the rats were allowed to swim in the pool for 90 seconds, and the time they spent in the target quadrant before the platform was removed was recorded by a video camera and analyzed using ETHOVISION XT (NOLDUS, version 4.1).

Statistical Analyses

IBM SPSS Statistics version 20.0 was used for the analyses. Results were expressed as mean ± standard error. The significance level was set at $p<0.05$. The Tukey test was used for pairwise comparisons following ANOVA when group variances were homogeneous and the data were approximately normally distributed. For groups that were not normally distributed and that exhibited heterogeneous variances, the Kruskal-Wallis test was used, followed by pairwise comparisons using the Mann-Whitney U test. Tukey's test was used for pairwise comparisons, and repeated-measures ANOVA was used for MWM and body weight data.

Results

Bodyweights

Body weight increased significantly in all groups over 5 weeks [$F(8,72)=9.6$ $p<0.001$]. However, there were no significant differences between groups across all weeks [$F(2,18)=2.8$ $p=0.08$].

Infarct area

The representative brain cross-sections in Figure 1 demonstrate that the infarcts were successfully established and show the observed effect of PRP therapy. Assessments of the infarct area in the early and late periods showed significant differences between the groups ($H(2,14)=7.1$ $p=0.02$, $H(2,14)=11.1$ $p=0.004$, respectively) A significant increase in the infarct area was found in the HIE group compared with the sham group in both the early and late periods ($U=2.5$, $p=0.01$; $U=0.0$, $p<0.001$, respectively). While no significant difference was found

between the PRP and HIE groups in the infarct area during the early period (U=4.5, p=0.17), a significant decrease was found in the infarct area during the late period (U=0.0, p=0.01) (Figures 2a, 2b). PRP significantly reduced the infarct size, particularly in the late period.

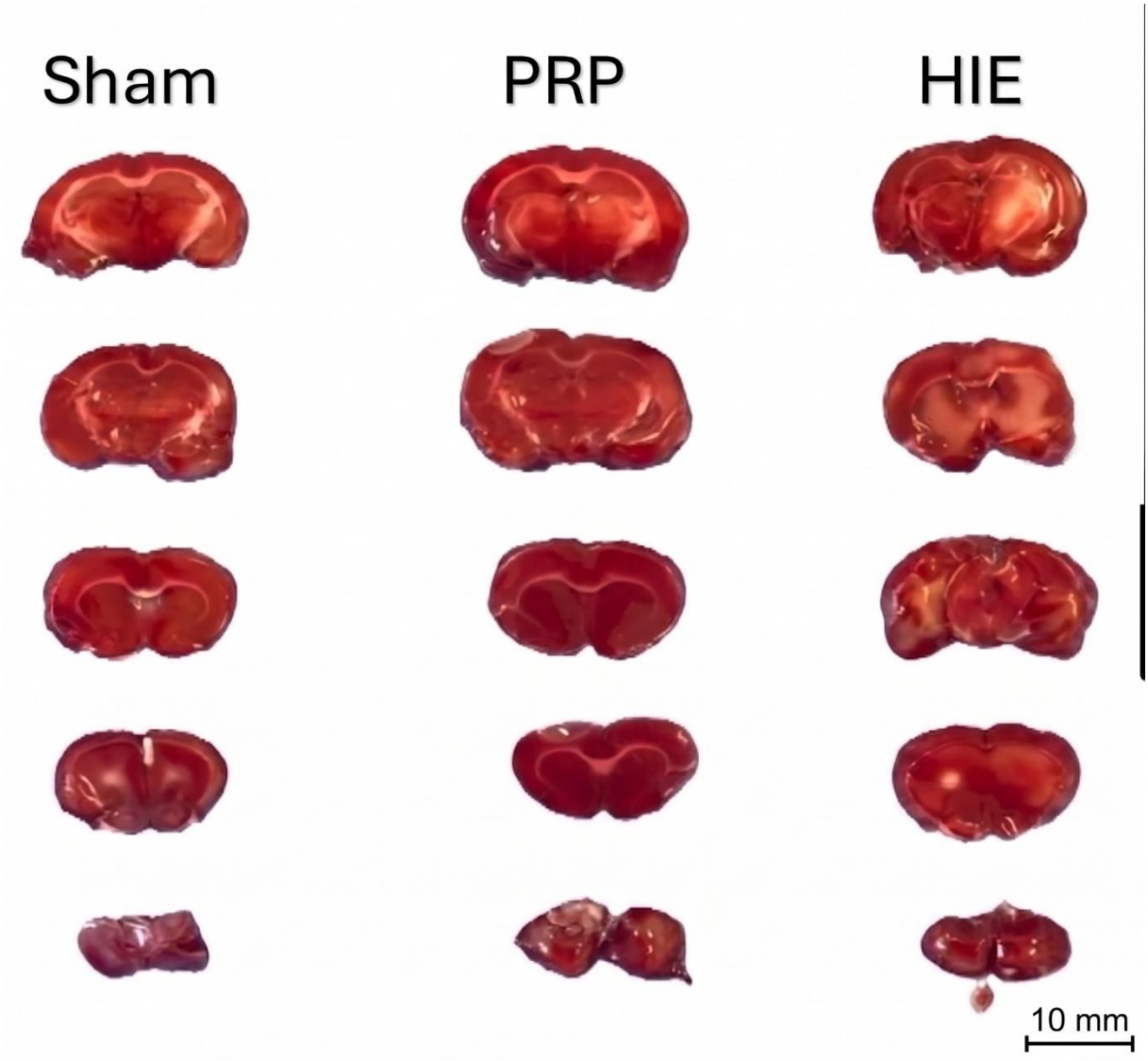


Fig. 1 The early period infarct areas of the groups

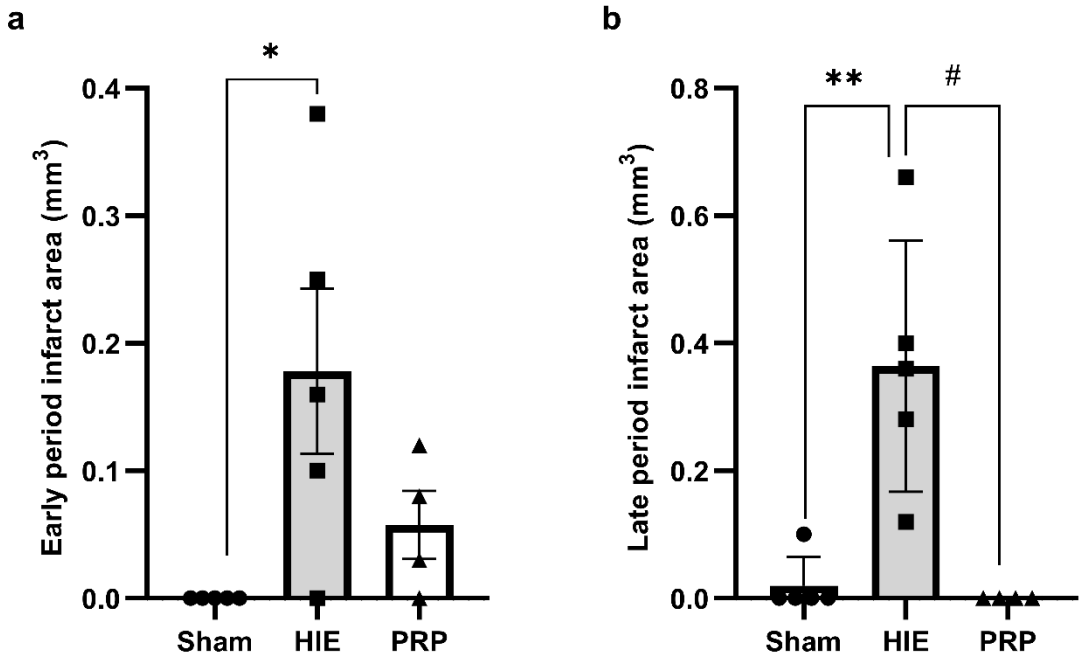


Fig. 2 Infarct area (a) early period, (b) late period. *p<0.05, **p<0.001 compared to the sham group, #p<0.05 compared to the HIE group. Kruskal-Wallis followed by Mann-Whitney U (n=4-5 per group, data presented as mean ± standard error)

TUNEL staining

During the early period, TUNEL staining revealed a significant difference between groups in the number of TUNEL-positive cells in brain tissue [H (2,14) = 8.7, p = 0.013]. The number of TUNEL-positive cells was significantly higher in the HIE group than in the sham group (U = 0.5, p = 0.01). However, no significant difference was found between the PRP and HIE groups (p > 0.05) (Figure 3a).

During the late period, a significant difference in TUNEL-positive cell counts was also found between the groups [H (2,14) = 9.2, p = 0.01]. The HIE group showed a significantly greater number of TUNEL-positive cells than the sham group (U = 0.0, p = 0.009). Furthermore, the number of TUNEL-positive cells was significantly lower in the PRP group than in the HIE group (U = 0.0, p = 0.01) (Figure 3b). Although PRP was associated with a numerical reduction in TUNEL-positive cells during the early period, this difference was not statistically significant; the reduction was significant during the late period. Representative photomicrographs of TUNEL-positive apoptotic cells and IL-1β immunoreactivity in the cerebral cortex are shown in Figure 4.

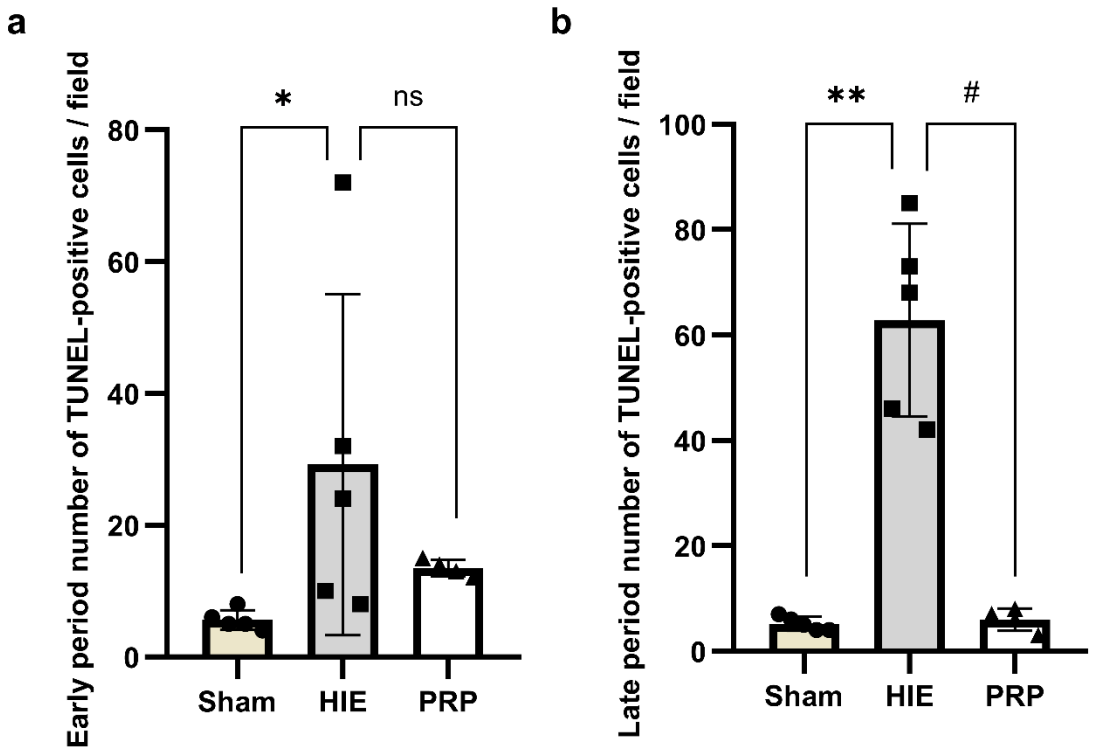


Fig. 3 Quantitative analysis of TUNEL staining during the early (72-hour) and late (42-day) periods. Data presented as mean ± standard error. Quantitative data are expressed as the number of TUNEL-positive neurons. *$p < 0.05$ and **$p < 0.01$ compared with the sham group; #$p < 0.05$ compared with the HIE group. Kruskal-Wallis test followed by Mann-Whitney U tests for pairwise comparisons (n=4-5 per group, ns; not significant)

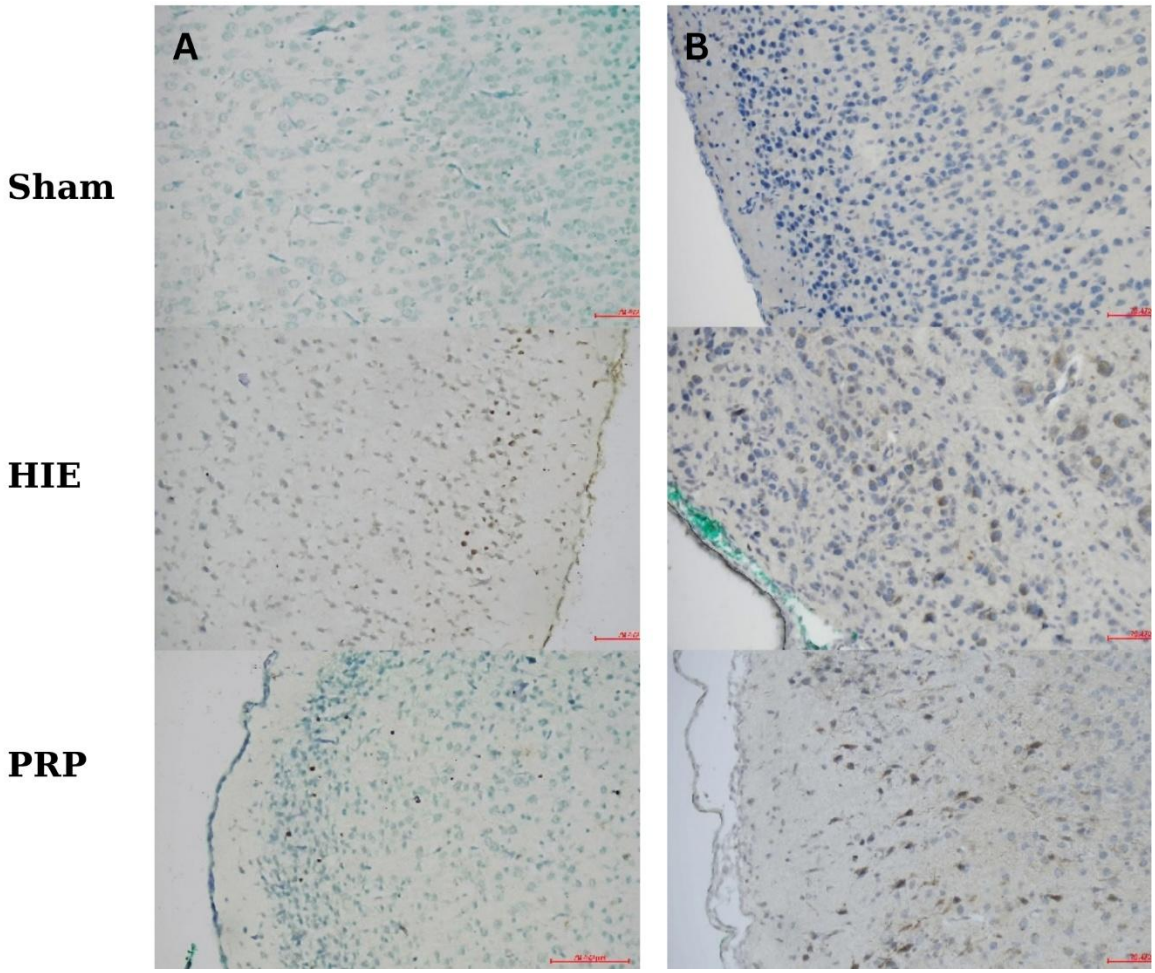


Fig. 4 Representative photomicrographs showing (A) TUNEL-positive apoptotic cells and (B) IL-1β immunoreactivity across the experimental groups (Sham, HIE, and PRP). In the Sham group, minimal or absent positive staining is observed for both markers. The HIE group shows a marked increase in TUNEL-positive apoptotic nuclei (brown stain) and elevated IL-1β expression compared to the Sham group. Treatment with PRP notably attenuates both apoptotic cell death (TUNEL) and inflammatory cytokine expression (IL-1β). (Scale bars =79.4 μm, magnification: 200×)

IL-1β staining

Significant differences between the groups in IL-1β staining percentage were found in the early and late periods (H (2,14)=11.2 p=0.004, H (2,14)=9.1 p=0.01, respectively). The percentage of IL-1β-staining areas was higher in the HIE group than in the sham group during both the early and late periods (U=0.0, p=0.008; U=0.0, p=0.009, respectively). However, IL-1β-staining areas decreased significantly in the PRP group compared with the HIE group during both the early and late periods (U=0.5, p=0.01; U=0.0, p=0.01, respectively) (Figure 5). The high levels of IL-1β staining in the HIE group indicate successful establishment of the hypoxic-ischemic model. PRP reduced neuroinflammation in both the early and late periods.

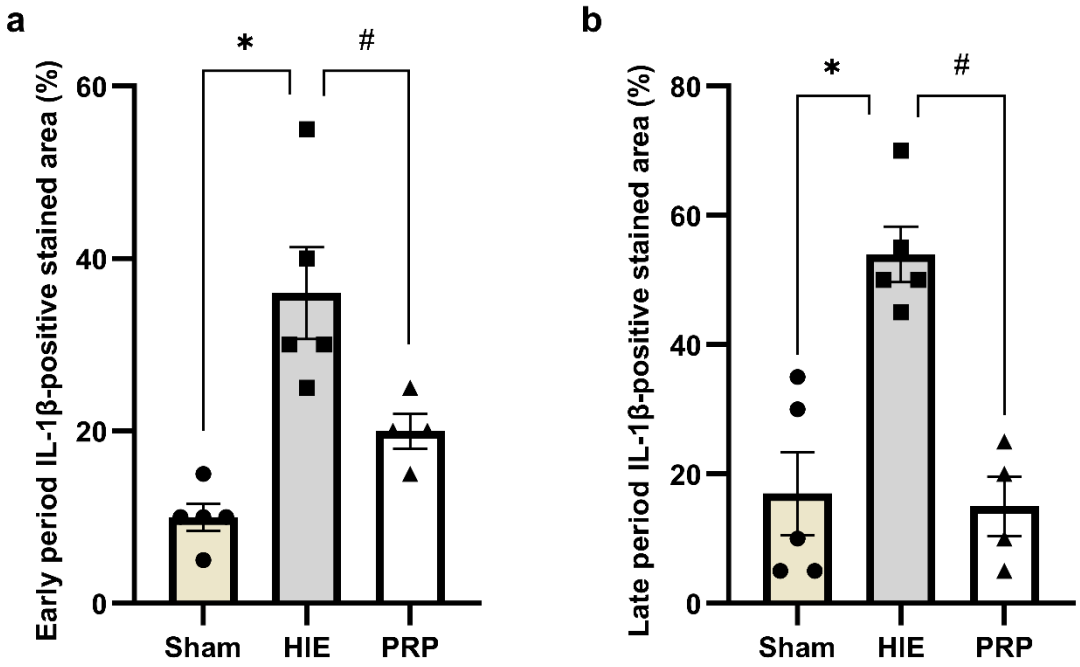


Fig. 5 Quantitative analysis and representative photomicrographs of IL-1β immunohistochemical staining during the early (72-hour) and late (42-day) periods. IL-1β immunoreactivity was quantified as the percentage of positively stained area within the selected peri-infarct region. *$p < 0.01$ compared with the sham group; #$p < 0.05$ compared with the HIE group. Kruskal-Wallis test followed by Mann-Whitney U tests for pairwise comparisons. Data presented as mean ± standard error (n=4-5 per group)

Open Field Test

The OF test was utilized to evaluate differences in locomotor activity and anxiety-like behaviors. A significant difference among groups was observed in time spent at the center area [F (2,18)=7.5, p=0.04]. The HIE group spent significantly less time in the central area than the sham group did (p=0.03). Additionally, time spent in the central area was significantly higher in the PRP group than in the HIE group (p=0.004) (Figure 6).

A significant difference was found among groups in entry time to the center [F (2,18)=5.6 p=0.01]. Latency to enter the center in the HIE group was significantly prolonged compared to the sham group (p=0.04). In addition, the PRP group's central latency time was significantly lower than the HIE group's (p=0.016).

The groups differed significantly in total distance traveled [F (2,18)=8.3 p=0.03]. There was no significant difference in the distance traveled between the HIE and sham groups. (p>0.05). However, the PRP group exhibited a significant increase in total distance traveled compared with the HIE group (p=0.002).

There was a significant difference in the frequency of center crossings [F (2,18)=8.4 p=0.01]. No significant difference was found in the frequency of center crossings between the HIE and sham groups. (p>0.05). However, the PRP group showed a significant increase in the frequency of center crossings compared with the HIE group (p=0.002).

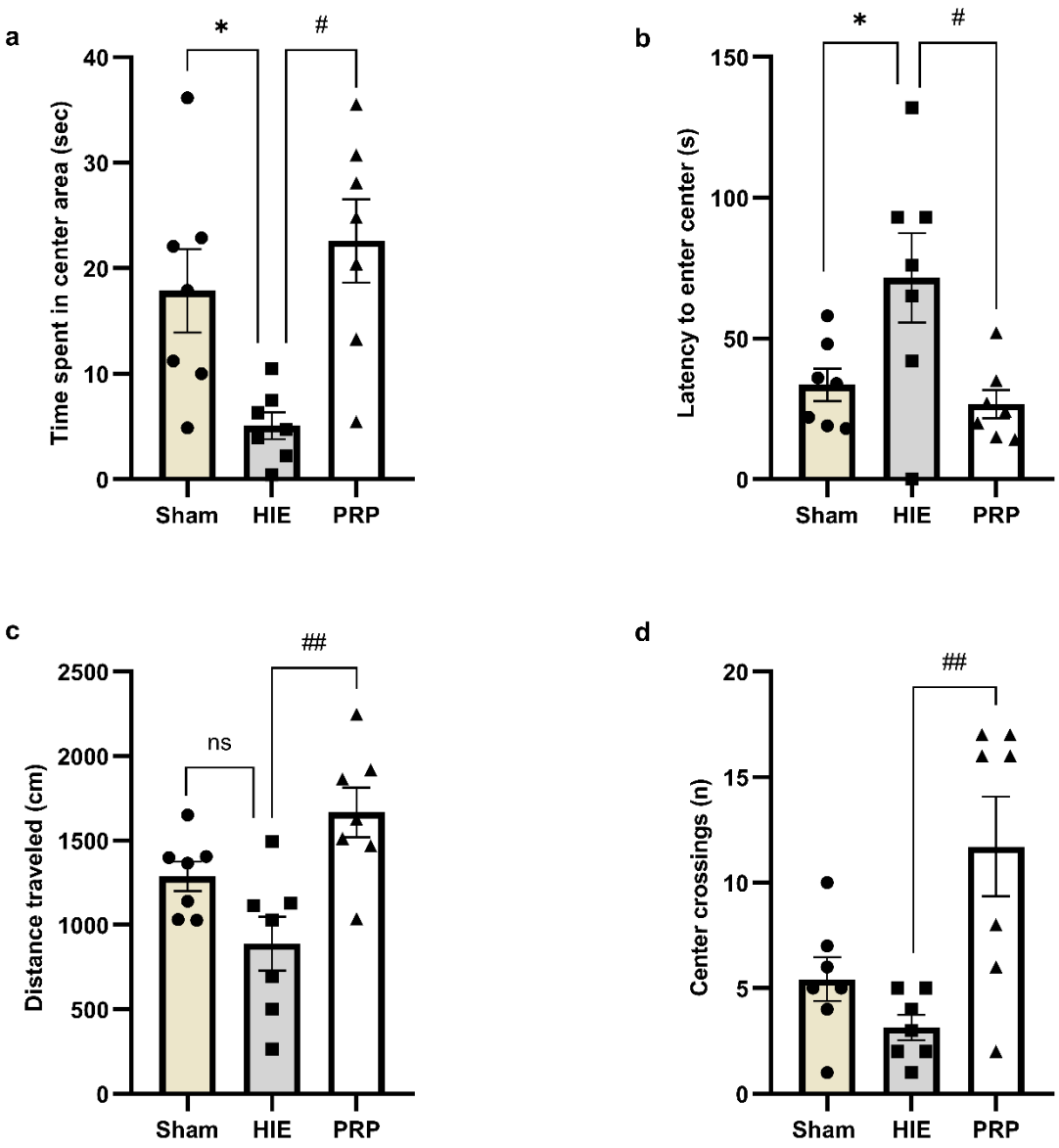


Fig. 6 Graphical representation of the trials conducted in the OF test. (a) Time spent in the central area during the OF (sec). *p<0.05 compared to the sham group, #p<0.01 compared to the HIE group, (n=7). (b) Time of central latency (seconds). *p<0.05 compared to the sham group, #p<0.05 compared to the HIE group, (n=7). (c) Distance traveled. ##p<0.01 compared to the HIE group, (n=7), ns: not significant. (d) Frequency of center crossing. ##p<0.01 compared to the HIE group, (n=7). Data presented as mean ± standard error. Tukey's test for pairwise comparisons following ANOVA

Morris water maze test

The MWM test was used to evaluate memory and spatial learning. Over the five training days, the groups showed a significant decrease in the time spent finding the platform [F (4,324)=32.2 p<0.001]. A significant difference was found between groups in the training trials [F (2,81)=11.8 p<0.001]. In the PRP group, the platform-finding time significantly increased on the second, third, and fourth days compared to the sham group

(p=0.04, p=0.003, and p=0.01, respectively). Additionally, on the third day, the PRP group showed a significant increase compared with the HIE group ($p<0.001$). In the MWM training trials, no significant differences in swimming speed were found between groups [$F(2,81)=2.9$ $p=0.15$] (Figures 7a, 7b). On the sixth day of the MWM test, there were no significant differences between groups in the time spent in the target quadrant and swimming speed ([$F(2,18)=2.0$ $p=0.15$] [$F(2,18)=2.6$ $p=0.09$], respectively).

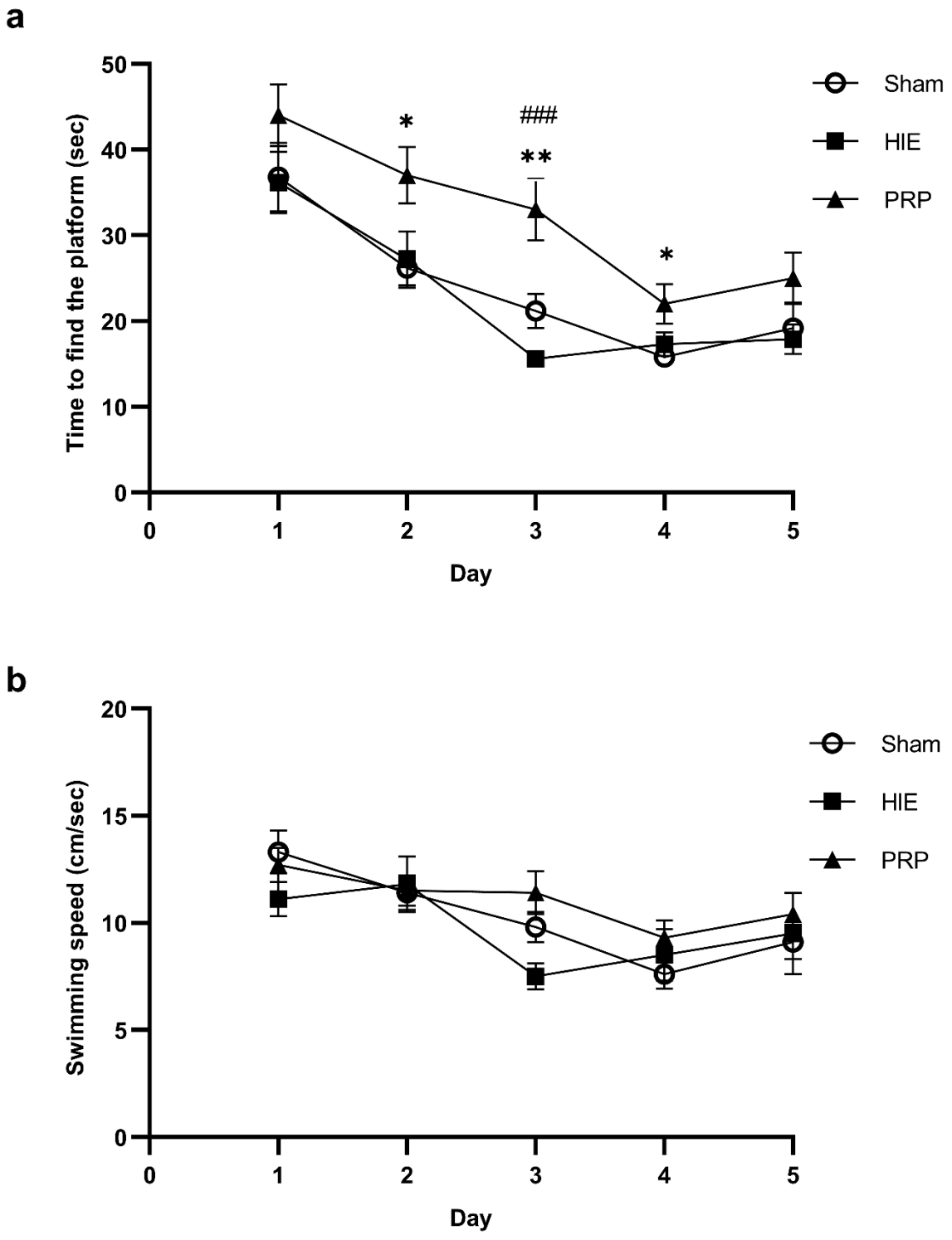


Fig. 7 MWM test: (a) platform finding time (seconds), (b) swimming speed. *p<0.05, **p<0.01 compared to the sham group, ###p<0.001 compared to the HIE group. Repeated measures ANOVA, Tukey test for pairwise comparisons. Data are presented as mean ± standard error. (n = 7 per group)

Discussion

This study sought to determine whether PRP treatment could mitigate neuroinflammation in newborn rats with HIE and to assess its long-term impact on neurological function. Although PRP therapy reduced the infarct area and the number of apoptotic cells in the early period, this effect was more significant in the late period. The increased percentage of IL-1β-stained areas in the HIE group indicates successful establishment of the HIE model. Furthermore, the reduction in IL-1β-stained areas with PRP treatment in both early and late periods indicates that it reduces neuroinflammation. Subsequent behavioral assessments indicated that elevated anxiety-like behavior in the HIE group decreased following PRP treatment. However, the MWM test also showed that PRP had no effect on cognitive functions.

Oxidative stress, inflammation, excitotoxicity, and energy deprivation–induced cell death (whether by apoptosis or necrosis) can all play a role in causing brain injury during HIE (Ranjan & Gulati, 2023). Subsequently, the resulting free oxygen radicals activate signaling pathways involved in the production of proinflammatory cytokines and chemokines such as IL-1β, IL-6, TNF, and interferons (IFNs), thereby triggering the inflammatory response and apoptosis (Ranneh et al., 2017). In a study evaluating the anti-inflammatory effect of PRP, it was demonstrated that it significantly inhibits the production of inflammatory factors, including IL-1β and TNF-α, in intervertebral disc degeneration (Akeda et al., 2019). Additionally, PRP has been found to reduce levels of proinflammatory cytokines (TNF-α, IL-1β, or IL-6) in an experimental model of arthritis (Tong et al., 2017). The anti-inflammatory properties and presence of various trophic factors in PRP have been shown to play an important role in the treatment of neurological disorders in several studies (Alcaraz et al., 2015; Anitua et al., 2015; Stolle et al., 2018; Wang et al., 2024). Thus, PRP therapy has been shown to reduce inflammation and promote neuronal survival in central nervous system models where neuroinflammation is a major factor, such as Parkinson's disease and stroke (Anitua et al., 2014; Borhani-Haghighi & Mohamadi, 2019; Zhang et al., 2015). In our study, PRP significantly decreased IL-1β levels, consistent with previous findings. However, this effect was particularly noticeable during the late period. The higher IL-1β staining observed at day 42 compared with day 3 in the HIE group is consistent with the concept of sustained tertiary neuroinflammation, whereby proinflammatory signaling may persist for weeks to months after the initial hypoxic-ischemic insult (Levison et al., 2022; Pedroza-García et al., 2022). In support of this interpretation, Wixey et al. reported persistent IL-1β elevation at postnatal day 45 in neonatal rats subjected to hypoxia-ischemia (Wixey et al., 2011), while Shrivastava et al. documented sustained cytokine expression for up to 21 days following neonatal hypoxia-ischemia in mice (Shrivastava et al., 2013). Activated resident microglia and infiltrating monocytes represent important cellular sources of IL-1β in the injured neonatal brain, and reactive astrocytes may also contribute to the sustained inflammatory response at later timepoints (Chen et al., 2022; Leavy & Jimenez Mateos, 2020; Levison et al., 2022; Pedroza-García et al., 2022). Importantly, the 72-hour and 42-day assessments in our study were performed in separate cohorts of animals (n = 5 and n = 7 per group, respectively), rather than as longitudinal measurements in the same animals. Therefore, direct numerical comparisons between the two timepoints should be interpreted cautiously, as inter-cohort variability in injury severity, litter effects, and regional susceptibility may contribute to the observed differences. Nevertheless, the significant attenuation of IL-1β staining in both the early and late periods following PRP administration supports a sustained anti-inflammatory effect of treatment and is consistent with the documented capacity of PRP-derived growth factors to suppress NF-κB-mediated inflammatory signaling (Anitua et al., 2015).

PRP stimulates neurogenesis, angiogenesis, cell survival and migration by activating platelet-derived growth factor (PDGF), insulin-like growth factor -1 (IGF-1), fibroblast growth factor (FGF), and vascular endothelial growth factor (VEGF), as well as some neurotrophic factors like nerve growth factor (NGF) and brain-derived neurotrophic factor (BDNF) (Kojima & Tator, 2002; Swift et al., 2006; Zhang et al., 2015). In a study investigating the effects of PRP on central nervous system cells, it was found to be efficient in ameliorating inflammation on microglia, decreasing apoptosis in neural progenitor cells, and maintaining neuronal synapses (Delgado et al., 2021). In another study that developed a neonatal HIE model, PDGF suppression resulted in a significant loss of neurons and inhibited neurite growth. It was concluded that suppression of PDGF induces neuronal apoptosis after neonatal cerebral hypoxia and ischemia by inhibiting P-PI3K and P-AKT signaling pathways (Xiong et al., 2019). Our research demonstrated that the anti-apoptotic activity of PRP was more pronounced during the late period; it also markedly reduced infarct areas at this stage. The lack of substantial efficacy during the early period may be due to increased blood-brain barrier permeability resulting from VEGF activity in PRP. The finding of a greater number of TUNEL-positive cells in the late period (day 42) than in the early period (day 3) may seem counterintuitive when considering only classical apoptosis, since caspase-dependent apoptosis following hypoxic-ischemic injury normally peaks within 24–72 hours (Pulera et al., 1998). A critical methodological consideration is that early and late assessments were carried out in different cohorts of animals (n = 5 and n = 7 per group, respectively) so that the numerical difference between timepoints does not reflect a longitudinal increase within the same animals. The same TUNEL staining protocol and quantification approach were used at both time points and the consistently low staining seen in the sham groups argues against a systematic staining artifact. Additionally, the late TUNEL signal is consistent with the tertiary phase of neurodegeneration in HIE, which can last for weeks to months after the initial injury and is characterized by ongoing neuroinflammation, mitochondrial dysfunction, oxidative stress, and neuronal loss (Levison et al., 2022; Pedroza-García et al., 2022). Importantly, TUNEL detects DNA strand breaks regardless of the mechanism involved and is therefore not specific for classical apoptosis. Other programmed cell death pathways, such as necroptosis and PARP-1-dependent parthanatos, and oxidative DNA damage can also lead to TUNEL-positive nuclei (Kari et al., 2022; Lear et al., 2025; Zhu et al., 2000). Therefore, the elevated TUNEL signal in the late period is likely to be due to a combination of continued secondary and tertiary neurodegeneration and non-apoptotic DNA damage, rather than simply the persistence of the acute apoptotic wave. The marked decrease in TUNEL-positive cells after PRP treatment in the late phase suggests that PRP may preferentially suppress mechanisms that contribute to this delayed phase of neuronal injury.

Multiple studies on the neuroinflammatory model of central nervous system disorders have shown that PRP exerts a neuroprotective effect on learning, memory, and synaptic plasticity by alleviating neuroinflammation and apoptosis (Bayat et al., 2020; Ji et al., 2023). The OF test, which is used to evaluate motor activity and anxiety-like behaviors, indicated that the HIE group spent less time in the central area and required more time to enter the central area. On the contrary, PRP administration reversed these effects, as evidenced by increased time spent in the central area, higher frequency of center crossings, greater total distance traveled, and a reduced latency to first entry to the central area. Collectively, these findings indicate that PRP treatment effectively ameliorates HIE-induced anxiety-like behavior. Additionally, the increased distance traveled by the PRP group compared with that of the HIE group indicates greater locomotor activity. The MWM test, which is conducted to

assess spatial learning and memory, revealed that cognitive functions were not affected, as no significant differences were found between the groups during the training trials or on the test day.

This study has several important limitations that must be addressed. A major limitation of this study is that it was not possible to demonstrate clearly the pathways through which growth and neurotrophic factors contained in PRP exert their effects. Due to the lack of cell-specific co-labeling, future studies should include a broader panel of cytokines (e.g., IL-6, TNF-α) to fully elucidate the inflammatory pathways involved. Another limitation of this study is the lack of evaluation regarding the efficacy of different PRP dosages and administration timings. Furthermore, it is important to acknowledge that the exclusion of female pups limits our ability to evaluate potential sex-dependent differences in neuroprotective responses to PRP. However, female rat pups were not included in the study because they might influence behavioral assessments during the transition to adulthood. Another limitation is that, because TUNEL staining detects DNA strand breaks regardless of the underlying cell death mechanism, it does not discriminate between classical caspase-3-mediated apoptosis and alternative programmed cell death pathways such as necroptosis or parthanatos (Kari et al., 2022; Zhu et al., 2000). Definitive characterization of the predominant cell death mechanisms — particularly at the late timepoint — would require complementary assays such as active caspase-3 immunolabeling or flow cytometry-based Annexin V staining. Additionally, IL-1β expression was quantified solely by immunohistochemistry, which is inherently semi-quantitative; complementary approaches such as enzyme-linked immunosorbent assay (ELISA) or quantitative reverse-transcription polymerase chain reaction (qRT-PCR) would allow more precise determination of protein and mRNA levels, respectively. Furthermore, the absence of co-labeling with cell-type-specific markers — such as ionized calcium-binding adaptor molecule 1 (Iba-1) for microglia or glial fibrillary acidic protein (GFAP) for astrocytes — precluded identification of the principal IL-1β-producing cell populations in the present model. Future studies incorporating cell-type-specific dual immunofluorescence labeling would also be valuable for determining the relative contributions of microglia, astrocytes, and neurons to the persistent IL-1β signal. Nevertheless, we believe that this is the first study to use PRP in a model of hypoxic-ischemic encephalopathy.

This study demonstrates that PRP therapy holds promising therapeutic potential for the management of HIE. However, further studies are required to elucidate the pathophysiological mechanisms underlying this therapeutic effect in HIE.

Declaration of generative AI and AI-assisted technologies in the manuscript preparation process

This work was prepared using AI and automated language tools solely for grammatical correction and paraphrasing. The authors reviewed and edited the content and take full responsibility for the content of the manuscript

References

Akeda, K., Yamada, J., Linn, E. T., Sudo, A., & Masuda, K. (2019). Platelet-rich plasma in the management of chronic low back pain: A critical review. *Journal of Pain Research*, *12*, 753–767. https://doi.org/10.2147/JPR.S153085

Alcaraz, J., Oliver, A., & Sánchez, J. M. (2015). Platelet-Rich Plasma in a Patient with Cerebral Palsy. *The American Journal of Case Reports*, *16*, 469–472. https://doi.org/10.12659/AJCR.893805

Anitua, E., Pascual, C., Antequera, D., Bolos, M., Padilla, S., Orive, G., & Carro, E. (2014). Plasma rich in growth factors (PRGF-Endoret) reduces neuropathologic hallmarks and improves cognitive functions in an Alzheimer's disease mouse model. *Neurobiology of Aging*, *35*(7), 1582–1595. https://doi.org/10.1016/j.neurobiolaging.2014.01.009

Anitua, E., Pascual, C., Pérez-Gonzalez, R., Orive, G., & Carro, E. (2015). Intranasal PRGF-Endoret enhances neuronal survival and attenuates NF-κB-dependent inflammation process in a mouse model of Parkinson's disease. *Journal of Controlled Release: Official Journal of the Controlled Release Society*, *203*, 170–180. https://doi.org/10.1016/j.jconrel.2015.02.030

Bayat, M., Zabihi, S., Karbalaei, N., & Haghani, M. (2020). Time-dependent effects of platelet-rich plasma on the memory and hippocampal synaptic plasticity impairment in vascular dementia induced by chronic cerebral hypoperfusion. *Brain Research Bulletin*, *164*, 299–306. https://doi.org/10.1016/j.brainresbull.2020.08.033

Borhani-Haghighi, M., & Mohamadi, Y. (2019). The therapeutic effect of platelet-rich plasma on the experimental autoimmune encephalomyelitis mice. *Journal of Neuroimmunology*, *333*, 476958. https://doi.org/10.1016/j.jneuroim.2019.04.018

Chen, H.-R., Chen, C.-W., Kuo, Y.-M., Chen, B., Kuan, I. S., Huang, H., Lee, J., Anthony, N., Kuan, C.-Y., & Sun, Y.-Y. (2022). Monocytes promote acute neuroinflammation and become pathological microglia in neonatal hypoxic-ischemic brain injury. *Theranostics*, *12*(2), 512–529. https://doi.org/10.7150/thno.64033

Delgado, D., Bilbao, A. M., Beitia, M., Garate, A., Sánchez, P., González-Burguera, I., Isasti, A., López De Jesús, M., Zuazo-Ibarra, J., Montilla, A., Domercq, M., Capetillo-Zarate, E., García del Caño, G., Sallés, J., Matute, C., & Sánchez, M. (2021). Effects of Platelet-Rich Plasma on Cellular Populations of the Central Nervous System: The Influence of Donor Age. *International Journal of Molecular Sciences*, *22*(4), 1725. https://doi.org/10.3390/ijms22041725

D'Hooge, R., & De Deyn, P. P. (2001). Applications of the Morris water maze in the study of learning and memory. *Brain Research. Brain Research Reviews*, *36*(1), 60–90. https://doi.org/10.1016/s0165-0173(01)00067-4

Douglas-Escobar, M., & Weiss, M. D. (2015). Hypoxic-ischemic encephalopathy: A review for the clinician. *JAMA Pediatrics*, *169*(4), 397–403. https://doi.org/10.1001/jamapediatrics.2014.3269

Emel, E., Ergün, S. S., Kotan, D., Gürsoy, E. B., Parman, Y., Zengin, A., & Nurten, A. (2011). Effects of insulin-like growth factor-I and platelet-rich plasma on sciatic nerve crush injury in a rat model. *Journal of Neurosurgery*, *114*(2), 522–528. https://doi.org/10.3171/2010.9.JNS091928

Festing, M. F. W. (2006). Design and Statistical Methods in Studies Using Animal Models of Development. *ILAR Journal*, *47*(1), 5–14. https://doi.org/10.1093/ilar.47.1.5

Jacobs, S. E., Berg, M., Hunt, R., Tarnow-Mordi, W. O., Inder, T. E., & Davis, P. G. (2013). Cooling for newborns with hypoxic ischaemic encephalopathy. *The Cochrane Database of Systematic Reviews*, *2013*(1), CD003311. https://doi.org/10.1002/14651858.CD003311.pub3

Jerez-Calero, A., Salvatierra-Cuenca, M. T., Benitez-Feliponi, Á., Fernández-Marín, C. E., Narbona-López, E., Uberos-Fernández, J., & Muñoz-Hoyos, A. (2020). Hypothermia Plus Melatonin in Asphyctic Newborns: A Randomized-Controlled Pilot Study. *Pediatric Critical Care Medicine: A Journal of the Society of Critical Care Medicine and the World Federation of Pediatric Intensive and Critical Care Societies*, *21*(7), 647–655. https://doi.org/10.1097/PCC.0000000000002346

Ji, L., Jin, R.-J., & Li, L. (2023). Platelet-rich Plasma Improves Radiotherapy-induced Emotional Disorder and Cognitive Dysfunction, Neuroinflammation in Aged Rats by Inhibiting the Activation of NLRP3 Inflammasomes. *Neurochemical Research*, *48*(8), 2531–2541. https://doi.org/10.1007/s11064-023-03933-9

Kari, S., Subramanian, K., Altomonte, I. A., Murugesan, A., Yli-Harja, O., & Kandhavelu, M. (2022). Programmed cell death detection methods: A systematic review and a categorical comparison. *Apoptosis: An International Journal on Programmed Cell Death*, *27*(7–8), 482–508. https://doi.org/10.1007/s10495-022-01735-y

Kojima, A., & Tator, C. H. (2002). Intrathecal Administration of Epidermal Growth Factor and Fibroblast Growth Factor 2 Promotes Ependymal Proliferation and Functional Recovery after Spinal Cord Injury in Adult Rats. *Journal of Neurotrauma*, *19*(2), 223–238. https://doi.org/10.1089/08977150252806974

Lear, B. A., McDouall, A. J., Lear, O. J., Dhillon, S. K., Lear, C. A., Northington, F. J., Bennet, L., & Gunn, A. J. (2025). The Potential Clinical Relevance of Necrosis–Necroptosis Pathways for Hypoxic–Ischaemic Encephalopathy. *Cells*, *14*(24), 1984. https://doi.org/10.3390/cells14241984

Leavy, A., & Jimenez Mateos, E. M. (2020). Perinatal Brain Injury and Inflammation: Lessons from Experimental Murine Models. *Cells*, *9*(12), 2640. https://doi.org/10.3390/cells9122640

Lee, A. C., Yu, V. M., Lowe, J. B., Brenner, M. J., Hunter, D. A., Mackinnon, S. E., & Sakiyama-Elbert, S. E. (2003). Controlled release of nerve growth factor enhances sciatic nerve regeneration. *Experimental Neurology*, *184*(1), 295–303. https://doi.org/10.1016/S0014-4886(03)00258-9

Levison, S. W., Rocha-Ferreira, E., Kim, B. H., Hagberg, H., Fleiss, B., Gressens, P., & Dobrowolski, R. (2022). Mechanisms of Tertiary Neurodegeneration after Neonatal Hypoxic-Ischemic Brain Damage. *Pediatric Medicine*, *5*, 28. https://doi.org/10.21037/pm-20-104

Luo, H., Zhang, Y., Zhang, Z., & Jin, Y. (2012). The protection of MSCs from apoptosis in nerve regeneration by TGFβ1 through reducing inflammation and promoting VEGF-dependent angiogenesis. *Biomaterials*, *33*(17), 4277–4287. https://doi.org/10.1016/j.biomaterials.2012.02.042

Miura, S., Ishida, A., Nakajima, W., Ohmura, A., Kawamura, M., & Takada, G. (2006). Intraventricular ascorbic acid administration decreases hypoxic–ischemic brain injury in newborn rats. *Brain Research*, *1095*(1), 159–166. https://doi.org/10.1016/j.brainres.2006.04.045

Nouraee, C., Fisher, M., Di Napoli, M., Salazar, P., Farr, T. D., Jafarli, A., & Divani, A. A. (2019). A Brief Review of Edema-Adjusted Infarct Volume Measurement Techniques for Rodent Focal Cerebral Ischemia Models with Practical Recommendations. *Journal of Vascular and Interventional Neurology*, *10*(3), 38–45.

Pedroza-García, K. A., Calderón-Vallejo, D., & Quintanar, J. L. (2022). Neonatal Hypoxic-Ischemic Encephalopathy: Perspectives of Neuroprotective and Neuroregenerative Treatments. *Neuropediatrics*, *53*(6), 402–417. https://doi.org/10.1055/s-0042-1755235

Perlman, J. M., Davis, P., Wyllie, J., & Kattwinkel, J. (2010). Therapeutic hypothermia following intrapartum hypoxia-ischemia. An advisory statement from the Neonatal Task Force of the International Liaison Committee on Resuscitation. *Resuscitation*, *81*(11), 1459–1461. https://doi.org/10.1016/j.resuscitation.2010.07.006

Pulera, M. R., Adams, L. M., Liu, H., Santos, D. G., Nishimura, R. N., Yang, F., Cole, G. M., & Wasterlain, C. G. (1998). Apoptosis in a Neonatal Rat Model of Cerebral Hypoxia-Ischemia. *Stroke*, *29*(12), 2622–2630. https://doi.org/10.1161/01.STR.29.12.2622

Ranjan, A. K., & Gulati, A. (2023). Advances in Therapies to Treat Neonatal Hypoxic-Ischemic Encephalopathy. *Journal of Clinical Medicine*, *12*(20), 6653. https://doi.org/10.3390/jcm12206653

Ranneh, Y., Ali, F., Akim, A. M., Hamid, H. A., & Et., A. (2017). Crosstalk between reactive oxygen species and pro-inflammatory markers in developing various chronic diseases: A review. *Applied Biological Chemistry*. https://doi.org/10.1007/s13765-017-0285-9

Rao, S. N. R., & Pearse, D. D. (2016). Regulating Axonal Responses to Injury: The Intersection between Signaling Pathways Involved in Axon Myelination and The Inhibition of Axon Regeneration. *Frontiers in Molecular Neuroscience*, *9*. https://doi.org/10.3389/fnmol.2016.00033

Reglodi, D., Tamás, A., Somogyvári-Vigh, A., Szántó, Z., Kertes, E., Lénárd, L., Arimura, A., & Lengvári, I. (2002). Effects of pretreatment with PACAP on the infarct size and functional outcome in rat permanent focal cerebral ischemia. *Peptides*, *23*(12), 2227–2234. https://doi.org/10.1016/S0196-9781(02)00262-0

Rice, J. E., Vannucci, R. C., & Brierley, J. B. (1981). The influence of immaturity on hypoxic-ischemic brain damage in the rat. *Annals of Neurology*, *9*(2), 131–141. https://doi.org/10.1002/ana.410090206

Rüegger, C. M., Davis, P. G., & Cheong, J. L. (2018). Xenon as an adjuvant to therapeutic hypothermia in near-term and term newborns with hypoxic-ischaemic encephalopathy. *The Cochrane Database of Systematic Reviews*, *8*(8), CD012753. https://doi.org/10.1002/14651858.CD012753.pub2

Sarnat, H. B., & Sarnat, M. S. (1976). Neonatal encephalopathy following fetal distress. A clinical and electroencephalographic study. *Archives of Neurology*, *33*(10), 696–705. https://doi.org/10.1001/archneur.1976.00500100030012

Semple, B. D., Blomgren, K., Gimlin, K., Ferriero, D. M., & Noble-Haeusslein, L. J. (2013). Brain development in rodents and humans: Identifying benchmarks of maturation and vulnerability to injury across species. *Progress in Neurobiology*, *106–107*, 1–16. https://doi.org/10.1016/j.pneurobio.2013.04.001

Shrivastava, K., Llovera, G., Recasens, M., Chertoff, M., Giménez-Llort, L., Gonzalez, B., & Acarin, L. (2013). Temporal Expression of Cytokines and Signal Transducer and Activator of Transcription Factor 3 Activation after Neonatal Hypoxia/Ischemia in Mice. *Developmental Neuroscience*, *35*(2–3), 212–225. https://doi.org/10.1159/000348432

Sondell, M., Lundborg, G., & Kanje, M. (1999). Vascular Endothelial Growth Factor Has Neurotrophic Activity and Stimulates Axonal Outgrowth, Enhancing Cell Survival and Schwann Cell Proliferation in the Peripheral Nervous System. *Journal of Neuroscience*, *19*(14), 5731–5740. https://doi.org/10.1523/JNEUROSCI.19-14-05731.1999

Stolle, M., Schulze, J., Roemer, A., Lenarz, T., Durisin, M., & Warnecke, A. (2018). Human Plasma Rich in Growth Factors Improves Survival and Neurite Outgrowth of Spiral Ganglion Neurons In Vitro. *Tissue Engineering. Part A*, *24*(5–6), 493–501. https://doi.org/10.1089/ten.TEA.2017.0120

Swift, M. J., Greene, J. A., Welch, Z. R., & Woodell-May, J. (2006). Concentration of Neurotransmitter and Neurotrophic Factors in Platelet Rich Plasma. *Blood*, *108*(11), 3914. https://doi.org/10.1182/blood.V108.11.3914.3914

Tong, S., Zhang, C., & Liu, J. (2017). Platelet-rich plasma exhibits beneficial effects for rheumatoid arthritis mice by suppressing inflammatory factors. *Molecular Medicine Reports*, *16*(4), 4082–4088. https://doi.org/10.3892/mmr.2017.7091

Tsuji, M., Sawada, M., Watabe, S., Sano, H., Kanai, M., Tanaka, E., Ohnishi, S., Sato, Y., Sobajima, H., Hamazaki, T., Mori, R., Oka, A., Ichiba, H., Hayakawa, M., Kusuda, S., Tamura, M., Nabetani, M., & Shintaku, H. (2020). Autologous cord blood cell therapy for neonatal hypoxic-ischaemic encephalopathy: A pilot study for feasibility and safety. *Scientific Reports*, *10*(1), 4603. https://doi.org/10.1038/s41598-020-61311-9

Victor, S., Rocha-Ferreira, E., Rahim, A., Hagberg, H., & Edwards, D. (2022). New possibilities for neuroprotection in neonatal hypoxic-ischemic encephalopathy. *European Journal of Pediatrics*, *181*(3), 875–887. https://doi.org/10.1007/s00431-021-04320-8

Wang, S., Liu, Z., Wang, J., Cheng, L., Hu, J., & Tang, J. (2024). Platelet-rich plasma (PRP) in nerve repair. *Regenerative Therapy*, *27*, 244–250. https://doi.org/10.1016/j.reth.2024.03.017

Wixey, J. A., Reinebrant, H. E., Spencer, S. J., & Buller, K. M. (2011). Efficacy of post-insult minocycline administration to alter long-term hypoxia-ischemia-induced damage to the serotonergic system in the immature rat brain. *Neuroscience*, *182*, 184–192. https://doi.org/10.1016/j.neuroscience.2011.03.033

Wu, Y. W., Comstock, B. A., Gonzalez, F. F., Mayock, D. E., Goodman, A. M., Maitre, N. L., Chang, T., Meurs, K. P. V., Lampland, A. L., Bendel-Stenzel, E., Mathur, A. M., Wu, T.-W., Riley, D., Mietzsch, U., Chalak, L., Flibotte, J., Weitkamp, J.-H., Ahmad, K. A., Yanowitz, T. D., … Juul, S. E. (2022).

Trial of Erythropoietin for Hypoxic–Ischemic Encephalopathy in Newborns. *New England Journal of Medicine*, *387*(2), 148–159. https://doi.org/10.1056/NEJMoa2119660

Xiong, L.-L., Xue, L.-L., Jiang, Y., Ma, Z., Jin, Y., Wang, Y.-C., Wang, Y.-Y., Xia, Q.-J., Zhang, Y., Hu, Q., Liu, J., & Wang, T.-H. (2019). Suppression of PDGF induces neuronal apoptosis after neonatal cerebral hypoxia and ischemia by inhibiting P-PI3K and P-AKT signaling pathways. *Brain Research*, *1719*, 77–88. https://doi.org/10.1016/j.brainres.2019.05.012

Zhang, Y., Ying, G., Ren, C., Jizhang, Y., Brogan, D., Liu, Z., Li, S., Ding, Y., Borlongan, C. V., Zhang, J., & Ji, X. (2015). Administration of human platelet-rich plasma reduces infarction volume and improves motor function in adult rats with focal ischemic stroke. *Brain Research*, *1594*, 267–273. https://doi.org/10.1016/j.brainres.2014.10.035

Zhu, C., Wang, X., Hagberg, H., & Blomgren, K. (2000). Correlation Between Caspase-3 Activation and Three Different Markers of DNA Damage in Neonatal Cerebral Hypoxia-Ischemia. *Journal of Neurochemistry*, *75*(2), 819–829. https://doi.org/10.1046/j.1471-4159.2000.0750819.x

Statements and Declarations

Ethical Approval: All protocols in this study were approved by the Medical and Experimental Research Center Ethics Committee at Çukurova University's Faculty of Medicine (approval number 2021-05).

Acknowledgments

We acknowledge the support of the Cukurova University Scientific Research Projects Coordination Unit

Disclosure This study was presented at the 32nd National Neonatology Congress held in Antalya, Türkiye, on 16-20 April 2025.

Financial support: Cukurova University Scientific Research Projects Coordination Unit (to N.Narli), project Nº TSA-2021-14224.

Authors' contributions

Tugay Tepe: Conceptualization, Methodology, Investigation, Writing-original draft, Project administration

Hacer Yapicioglu Yildizdas: Conceptualization, Methodology, Writing-original draft, Supervision

Kübra Akillioglu: Methodology, Investigation

Seda Köse: Methodology, Investigation

Seyda Erdogan: Methodology, Investigation, Formal analysis

Tugba Toyran: Methodology, Investigation, Formal analysis

Nejat Narli: Writing - original draft, Funding acquisition, Resources

Mehmet Satar: Supervision, Writing - review & editing

Conflicts of Interest: The authors have no conflicts of interests to declare that are relevant to the content of this article

Data Availability: Requests concerning data access should be directed to the authors

Supplementary Files

This is a list of supplementary files associated with this preprint. Click to download.

- ARRIVEChecklist.docx
- Graphicalabstract.png
- Highlights.docx